

Electronic Supplementary Information

Facile electrodeposition of V-doped CoP on vertical graphene for efficient alkaline water electrolysis

Linh Truong,^a Sanjib Baran Roy,^a Sahng-Kyoon Jerng,^b Jae Ho Jeon,^a Sunghun Lee^a and
Seung-Hyun Chun^c

^a Department of Physics, Sejong University, Seoul 05006, Korea

^b Graphene Research Institute, Sejong University, Seoul 05006, Korea

^c Corresponding Author: FAX: +82 2 3408 4316. E-mail address: schun@sejong.ac.kr (S. H. Chun)

Experimental section

1. Synthesis of VG/CC

The synthesis of VG was carried out by a plasma enhanced chemical vapor deposition (PECVD) system. A piece of CC ($6 \times 6 \text{ cm}^2$) was cleaned in acetone, deionized water and ethanol for 10 min by ultrasonic treatment, respectively, and was put into the PECVD reaction chamber. Prior to VG growth, the substrate was heated and when the temperature reached to $750 \text{ }^\circ\text{C}$, H_2 plasma (20 sccm) was generated by a radio frequency power of 50 W at a chamber pressure of 10 Torr for 2 min to remove unintended contaminants from the CC surface. After this treatment, CH_4 (10 sccm) and H_2 (20 sccm) plasma were continuously generated into the reaction chamber for 45 min to grow VG of an average height around 15 nm.

2. Synthesis of V-CoP/VG/CC

In a typical synthesis, VCl_3 (5 mM, 10 mM, and 15 mM) was loaded into a beaker containing the dissolved solution of 80 ml deionized water, 50 mM $\text{CoSO}_4 \cdot 7 \text{ H}_2\text{O}$, 0.5 M NaH_2PO_2 and 0.1 M CH_3COONa under 500 rpm stirring for 2 min to form a deposition electrolyte. A $1 \times 1 \text{ cm}^2$ of VG/CC as working electrode was exposed to the deposition solution. A graphite rod and an Ag/AgCl (sat. KOH) were used as counter and reference electrodes, respectively. The experiment was conducted at room temperature with different applied current densities (-0.05 and -0.1 A cm^{-2}) for 10 min. After deposition, the product was rinsed carefully in deionized water and dried at room temperature. For comparison, CoP/VG/CC was prepared under the optimized condition reported previously ¹.

3. Electrocatalytic measurements

All electrochemical tests were carried out on a Biologic SP-300 workstation using a standard three-electrode electrochemical cell with a graphite rod as a counter electrode, a Hg/HgO (1.0 M NaOH) as a reference electrode. A geometric area of 0.6 cm^2 of V-CoP/VG/CC was exposed to 1.0 M KOH solution and performed as a working electrode to collect its

polarization curves at a scan rate of 10 mV s^{-1} . For comparison, Pt/C and IrO_2 were tested as HER and OER benchmark catalysts, respectively. Prior to oxygen evolution measurement, the electrolyte was purged with highly pure oxygen gas for 20 min. Moreover, all reported potentials were calibrated to RHE scale by the following equation, $E (\text{vs. RHE}) = E (\text{vs. Hg/HgO}) + E^0(\text{Hg/HgO}) + 0.059 \times \text{pH}$. Polarization curves were corrected by iR compensation in 1.0 M KOH. The C_{dl} values were obtained by performing CV measurements at different scan rates.

S1. Influence of configuration of substrate on the morphology of V-CoP

Fig. S1 showed SEM images of CC, VG grown on CC, V-CoP deposited on CC surface and V-CoP deposited on VG/CC surface. As observed, the V-CoP nanoparticles were formed on CC substrate (Fig. S1 c) while the cauliflower-like structure of V-CoP were formed on VG/CC substrate. Obviously, the rougher surface of V-CoP/VG/CC could provide the catalytic sites which is beneficial for the catalytic activities.

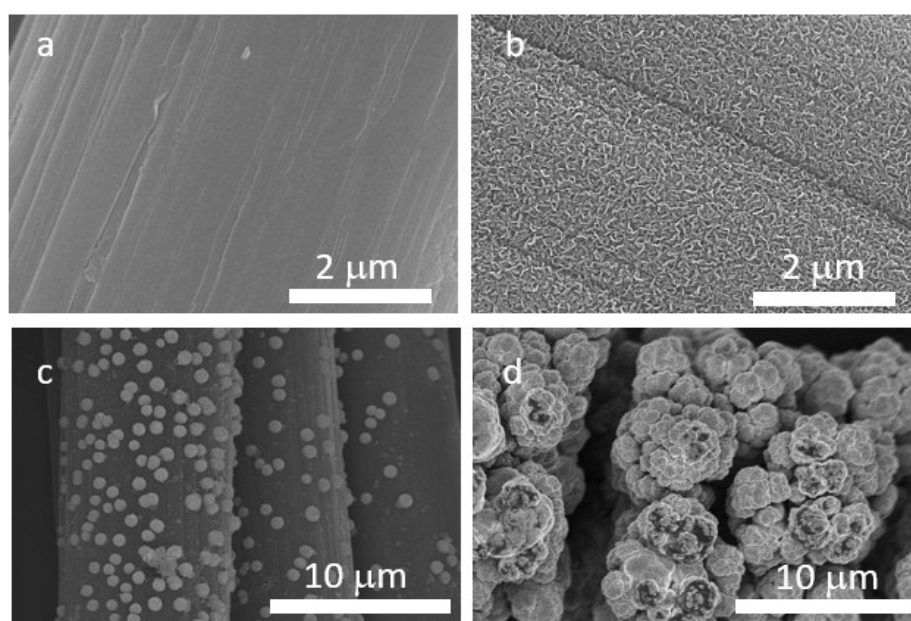


Fig. S1. SEM images of (a) CC, (b) VG/CC, (c) V-CoP/CC, and (d) V-CoP/VG/C

S2. Influence of concentration of vanadium in electrodeposition solution on the morphology of V-CoP on VG/CC

The different amounts of vanadium reagent (5, 10 and 15 mM) added into the electrodeposition electrolyte induced the different morphologies of V-CoP on VG/CC surface. Fig S2 showed the morphologies of V-CoP/VG/CC with 5 and 15 mM vanadium reagents. Notably, the microsphere structure (around 5 μm) of V-CoP were observed.

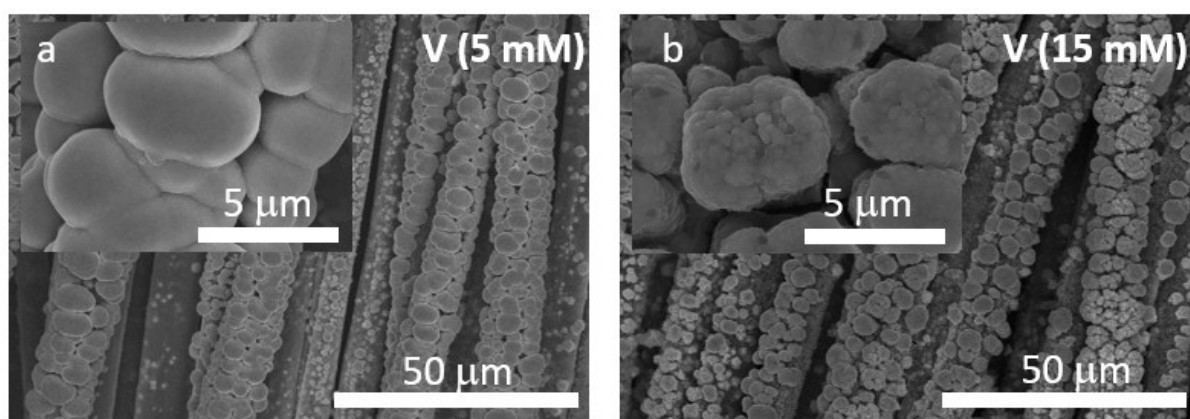


Fig. S2. Low- and high- magnifications (inset) SEM images of V-CoP/VG/CC with 5 mM and 15 mM vanadium.

S3. Energy dispersive spectroscopy spectrum of V-CoP/VG/CC

The surface of as-prepared V-CoP/VG/CC was composed by a considerable amount of cobalt, which generally observed from the electrodeposition method. The 10 cycles of HER of V-CoP/VG/CC (5 mM vanadium) was conducted in acidic medium prior to the EDS measurement to yield a CoP stoichiometric ratio of 1 : 1. The EDS result indicated that V : Co : P atomic ratio is 0.4 : 9.8 : 10.3 for V-CoP/VG/CC (5 mM vanadium).

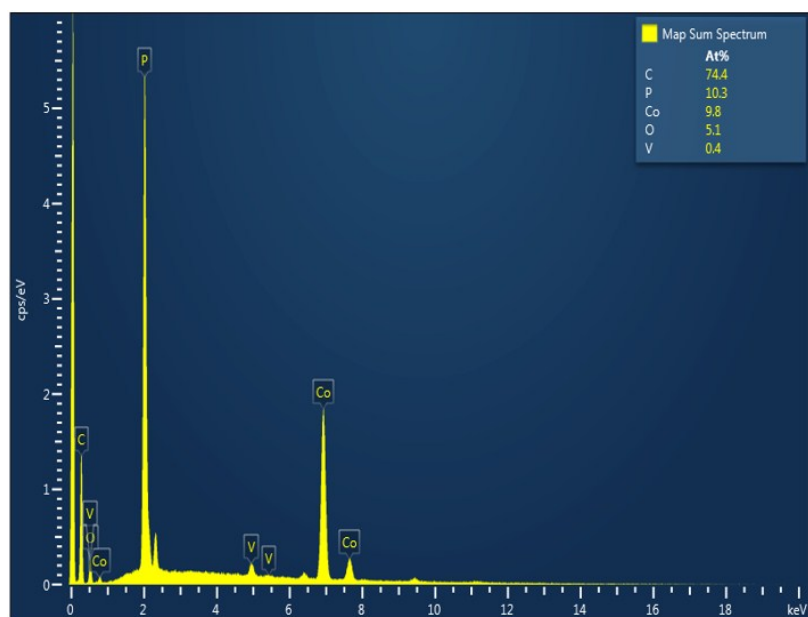


Fig. S3. The energy spectroscopy spectrum (EDS) spectra of V-CoP/VG/CC (5 mM vanadium) after the catalytic reactions.

S4. XPS spectra of as-prepared V-CoP/VG/CC

The C 1s spectra of V-CoP/VG/CC indicated three peaks at 284.6 eV, 286.0 eV, and 288.0 eV corresponding to C-C, C-O, and C=O, respectively. Two main peaks at 778.7 eV and 782.3 eV and one satellite peak at 785.8 eV were detected in the Co 2p_{3/2} region. The Co 2p_{1/2} region indicated two main peaks at 793.8 eV and 798.4 eV and one satellite peak at 803.7 eV. In the P 2p spectra, the two main peaks at 129.7 eV and 130.5 eV were assigned to the P 2p_{3/2} and P 2p_{1/2} regions, respectively, and the orthophosphate peaks were at 133.6 eV and 134.5 eV.¹ The characteristic binding energies of Co metal at 778.7 eV and P at 129.7 eV correspond to the Co 2p_{3/2} and P 2p_{3/2} components in CoP nanocrystals.^{2,3} In the V 2p spectra, the peaks at the binding energies of 517.4 eV (V 2p_{3/2}) and 524.7 eV (V 2p_{1/2}) were attributed to V⁵⁺ of V-CoP/VG/CC.⁴

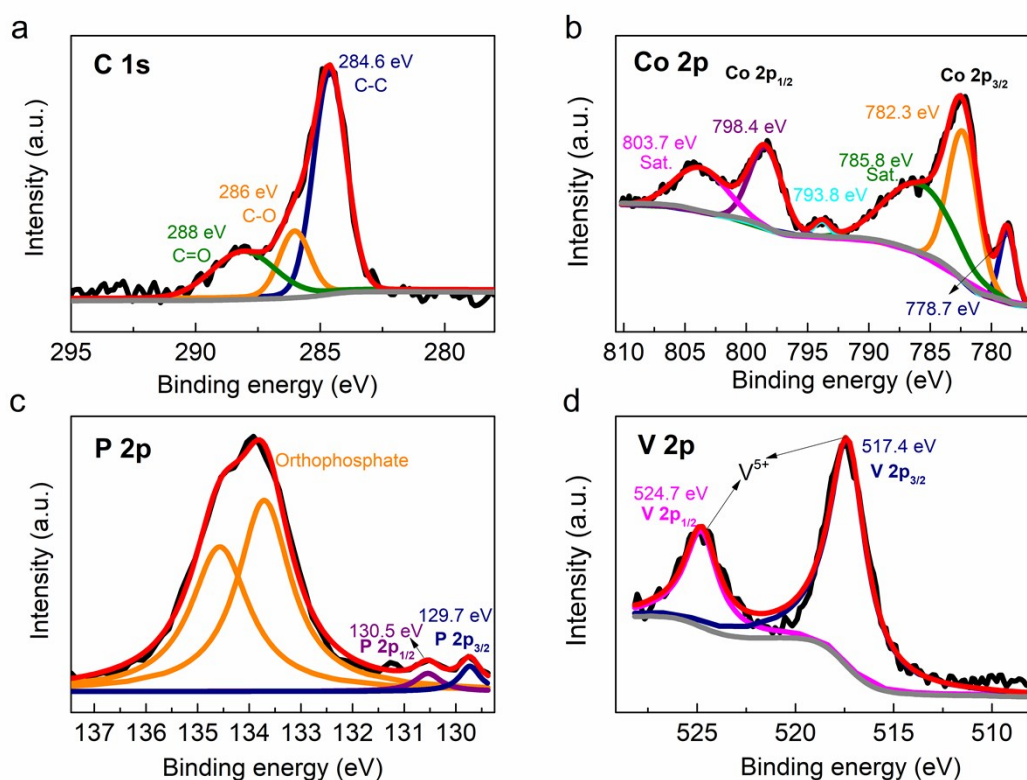


Fig. S4 XPS spectra of V-CoP/VG/CC structure in (a) C 1s, (b) Co 2p, (c) P 2p, and (d) V 2p regions.

S5. Electrochemical double-layer capacitance

The electrochemical double-layer capacitance (C_{dl}) is obtained by using cyclic voltammetry (CV) in the non-Faradaic regime performed under a series of different scan rates of 20, 30, 40, 50, 60, 70, 80, 90 and 100 mV s^{-1} (Figure S5a and S5c). The differences in variation of current density ($\Delta j = j_a - j_c$) at overpotential of 1.05 V vs. RHE as functions of the scan rate are plotted. These plotted lines are fitted by linear regression as shown in Fig S5b and S5d, and the slope value is twice C_{dl} .

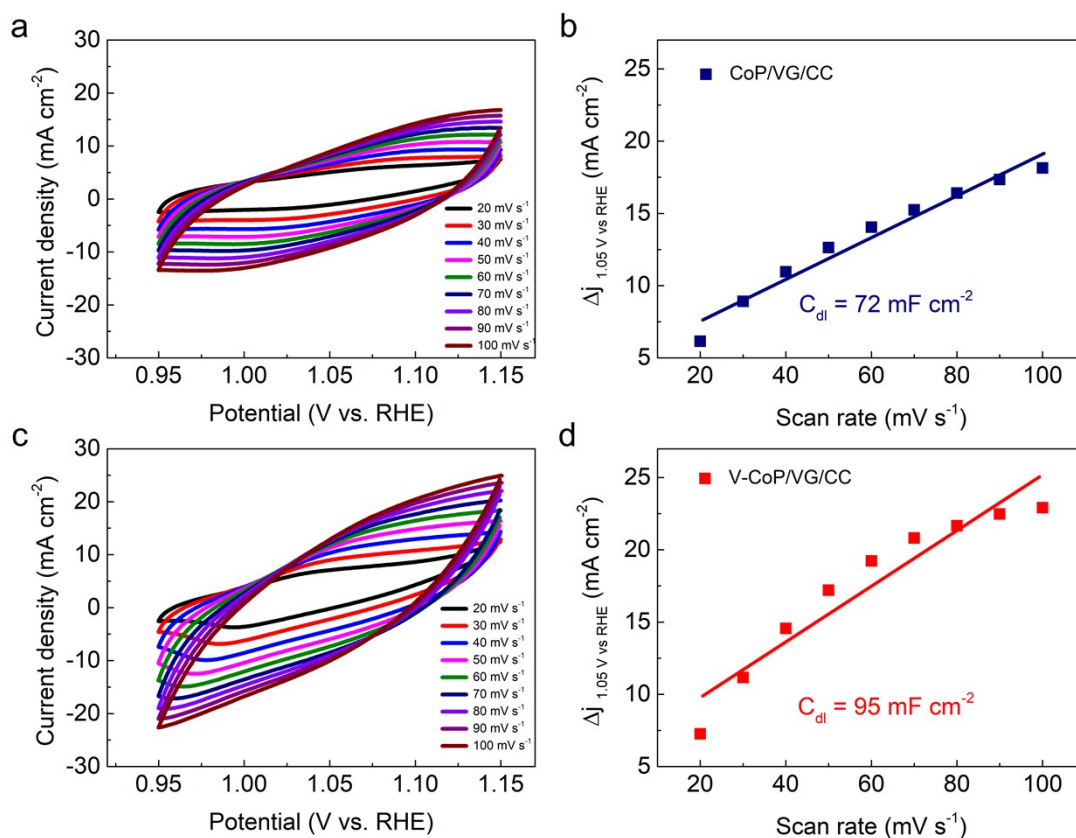


Fig. S5 Double layer capacitance (C_{dl}) measurements of CoP/VG/CC and V-CoP/VG/CC. Cyclic voltammograms at the scan rate range 20-100 mV/s within 0.95 to 1.15 V of (a) CoP/VG/CC, (c) V-CoP/VG/CC. The relationship between the current density change and the scan rate for (b) CoP/VG/CC, (d) V-CoP/VG/CC.

S6. Influence of electrodeposition current density on the HER and OER performances in 1.0 M KOH

We evaluated the HER and OER performances of as-prepared V-CoP/VG/CC deposited with the applied current densities of 0.1 A cm^{-2} and 0.05 A cm^{-2} . In view of the fact, the V-CoP/VG/CC - 0.1 A cm^{-2} displayed the better HER and OER in 0.1 M KOH , we thus set it as an optimized condition for following discussion.

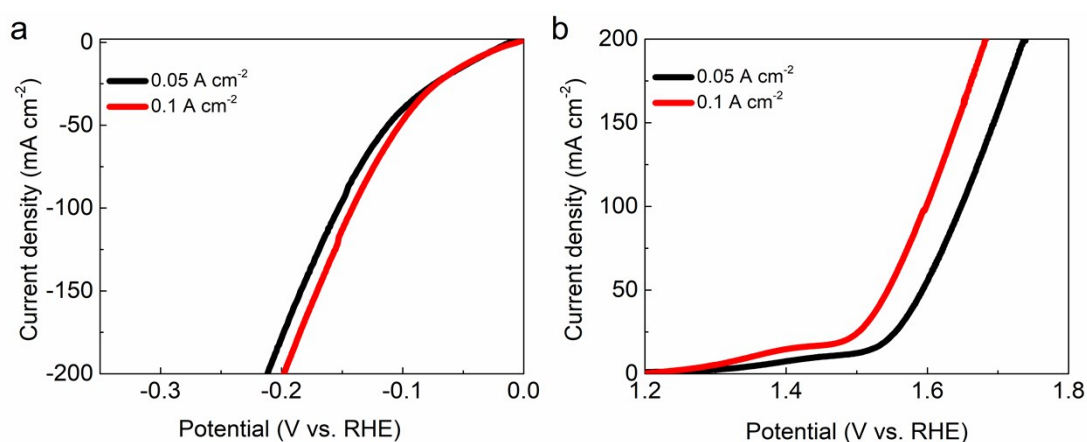


Fig. S6. The influence of the electrodeposition current density of 0.05 A cm^{-2} and 0.1 A cm^{-2} on (a) HER and (b) OER performances of V-CoP/VG/CC, deposited with an addition of 10 mM VCl_3 .

S7. Influence of vanadium concentration on the HER and OER performance in 1.0 M

KOH

We evaluated the HER and OER performances of as-prepared V-CoP/VG/CC deposited with the applied current densities of 0.1 A cm^{-2} and 0.05 A cm^{-2} . In view of the fact, the V-CoP/VG/CC - 0.1 A cm^{-2} displayed the better HER and OER in 0.1 M KOH , we thus set it as an optimized condition for following discussion.

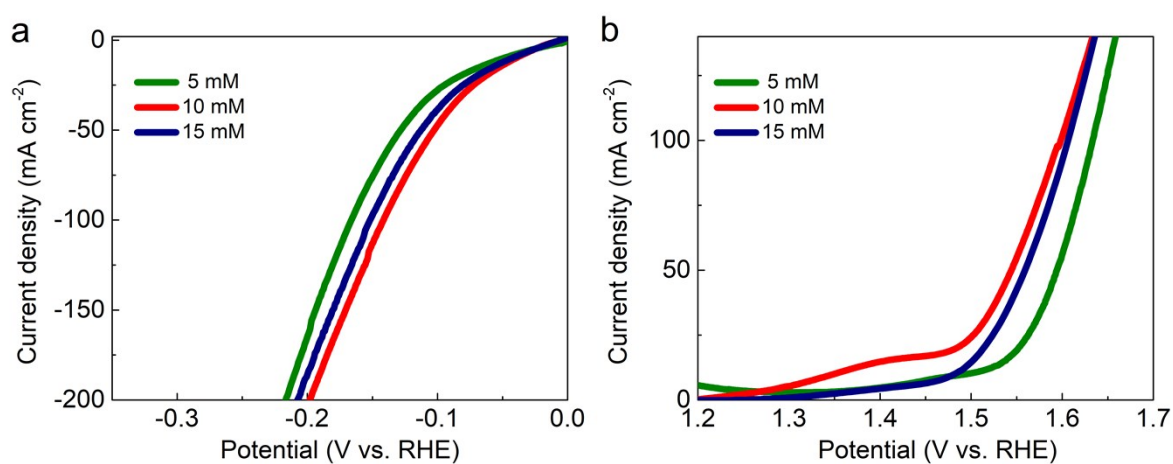


Fig. S7 The influence of vanadium concentration (5 mM, 10 mM, and 15 mM) on (a) HER and (b) OER performances of V-CoP/VG/CC deposited with the same applied current density 0.1 A cm^{-2} .

S8. Comparison table of electrocatalytic performances in alkaline medium (1.0 M KOH) for V-CoP/VG/CC with other electrocatalysts (Table S1)

Ref	Material and structure feature	j (mA cm ⁻²)	η_{HER} (mV)	η_{OER} (mV)	The cell voltage (V) for OWS
5	Fe doped Ni ₂ P nanosheet arrays	10	-	-	1.49
		50	213	230	~1.68
6	3D porous amorphous γ -CrOOH/NF	10	-	-	1.56
		50	149	334	~1.76
7	Hydrotalcite-like Ni(OH) ₂ nanosheets/NF	10	127	170	1.68
		50	237	330	~1.86
8	NiS microsphere film/NF	10	~140	-	1.64
		50	~200	335	~1.81
9	Ni-P nanoparticles film/CF	10	98	325	1.68
		50	-	~390	~1.82
10	NiMo hollow nanorod array/Ti mesh	10	92	310	1.64
		50	-	~340	~1.83
11	Hollow CoP nanoparticle/ N-doped graphene	10	83	262	1.58
		50	-	~330	~1.69
12	Mn-CoP microcubes/rGO	10	54	250	1.55
		50	-	~300	~1.68
	This work	10	40	-	-
		50	103	314	1.69

j : current density; η_{HER} : overpotential for hydrogen evolution reaction; η_{OER} : overpotential for oxygen evolution reaction; OWS: overall water splitting; NF: nickel foam; CF: copper foam; CC: carbon cloth; rGO: reduced graphene oxide

“~” denoted the estimated value from the graph shown in the literature; “-” denoted the value is not presented on the literature.

References

- 1 L. Truong, S.-K. Jerng, S. B. Roy, J. H. Jeon, K. Kim, K. Akbar, Y. Yi and S.-H. Chun, *ACS Sustain. Chem. Eng.*, 2019, **7**, 4625–4630.
- 2 M. Li, X. Liu, Y. Xiong, X. Bo, Y. Zhang, C. Han and L. Guo, *J. Mater. Chem. A*, 2015, **3**, 4255–4265.
- 3 X. Yang, A.-Y. Lu, Y. Zhu, M. N. Hedhili, S. Min, K.-W. Huang, Y. Han and L.-J. Li, *Nano Energy*, 2015, **15**, 634–641.
- 4 X. Xiao, L. Tao, M. Li, X. Lv, D. Huang, X. Jiang, H. Pan, M. Wang and Y. Shen, *Chem. Sci.*, 2018, **9**, 1970–1975.
- 5 Y. Li, H. Zhang, M. Jiang, Q. Zhang, P. He and X. Sun, *Adv. Funct. Mater.*, 2017, **27**, 1702513.
- 6 Z. Sun, M. Yuan, H. Yang, L. Lin, H. Jiang, S. Ge, H. Li, G. Sun, S. Ma and X. Yang, *Inorg. Chem.*, 2019, **58**, 4014–4018.
- 7 Y. Rao, Y. Wang, H. Ning, P. Li and M. Wu, *ACS Appl. Mater. Interfaces*, 2016, **8**, 33601–33607.
- 8 W. Zhu, X. Yue, W. Zhang, S. Yu, Y. Zhang, J. Wang and J. Wang, *Chem. Commun.*, 2016, **52**, 1486–1489.
- 9 Q. Liu, S. Gu and C. M. Li, *J. Power Sources*, 2015, **299**, 342–346.
- 10 J. Tian, N. Cheng, Q. Liu, X. Sun, Y. He and A. M. Asiri, *J. Mater. Chem. A*, 2015, **3**, 20056–20059.
- 11 X. Yu, S. Zhang, C. Li, C. Zhu, Y. Chen, P. Gao, L. Qi and X. Zhang, *Nanoscale*, 2016, **8**, 10902–10907.
- 12 X. Xu, H. Liang, G. Tang, Y. Hong, Y. Xie, Z. Qi, B. Xu and Z. Wang, *Nanoscale Adv.*, 2019, **1**, 177–183.